IEEE Access
Multidisciplinary | Rapid Review | Open Access Journal

Received 17 January 2024, accepted 31 January 2024, date of publication 5 February 2024, date of current version 20 February 2024.

Digital Object Identifier 10.1109/ACCESS.2024.3362241

RESEARCH ARTICLE

Optimal Design of a Grid-Independent Solar-Fuel Cell-Biomass Energy System Using an Enhanced Salp Swarm Algorithm Considering Rule-Based Energy Management Strategy

BABANGIDA MODU[1,2], MD. PAUZI BIN ABDULLAH[1,3], (Senior Member, IEEE), ABDULRAHMAN ALKASSEM[4], (Member, IEEE), HASSAN Z. AL GARNI[5], (Member, IEEE), AND MISHAAL ALKABI[6], (Member, IEEE)

[1]Centre of Electrical Energy Systems, Faculty of Electrical Engineering, Universiti Teknologi Malaysia (UTM), Skudai, Johor 81310, Malaysia
[2]Department of Electrical and Electronic Engineering, University of Maiduguri, Maiduguri, Borno 1069, Nigeria
[3]Institute of Future Energy, Universiti Teknologi Malaysia (UTM), Skudai, Johor 81310, Malaysia
[4]Department of Electrical Engineering, Faculty of Engineering, Islamic University of Madinah, Madinah 42351, Saudi Arabia
[5]Department of Electrical Engineering, Jubail Industrial College, Jubail 31961, Saudi Arabia
[6]Department of Electrical Engineering, Faculty of Engineering, Umm Al-Qura University, Makkah 24381, Saudi Arabia

Corresponding authors: Md. Pauzi Bin Abdullah (mpauzi@utm.my), Abdulrahman Alkassem (a.akassem@iu.edu.sa), and Babangida Modu (modu@graduate.utm.my)

ABSTRACT This paper presented an optimal design of a grid-independent hybrid renewable energy system (HRES) that comprises Photovoltaic, Biomass, Hydrogen Fuel Cell, and battery storage. Renewable energy-based system have been endorsed for remote off-grid communities electrification. However, it is difficult to design an optimal hybrid energy system due to the stochastic resource nature, load variation, and high cost of renewable components. The sizing of components for the proposed HRES is determined through the application of an innovative metaheuristic optimization technique called salp swarm algorithm (SSA). Addressing the limitations of the salp swarm algorithm, which include low precision, optimization dimension and convergence rate, a modified version of the salp swarm algorithm (SSA), known as the Levy and sine cosine operator-based (LSC-SSA), was introduced. The proposed algorithm is compared with standard SSA and Genetic Algorithm (GA). The primary goal of the research is to reduce the annualized cost of the hybrid system, whilst taking into account the reliability constraint. The novelty of this research lies in its approach to enhance the performance of a HRES by optimizing its size and energy management strategy (EMS). It is achieved by employing a combined framework that integrate the proposed LSC-SSA into the supervisory EMS. The potential benefits of this approach include reducing the cost of energy and the annualized system cost. The comparative results validate that the LSC-SSA surpasses the standard SSA, and GA algorithms examined, by realizing significant cost reductions amounting to $82,023, and $202,127 respectively. Additionally, the outcome indicates that, the LSC-SSA offers the least cost of energy (COE) of $0.927/kWh, in comparison with the COE values of $0.931/kWh for SSA and $0.949/kWh for GA, which are higher. Furthermore, the results indicate that the applied supervisory EMS has effectively assisted the establishing an eco-friendly and economical energy system.

INDEX TERMS Solar PV, biomass, fuel cell, rule-based, energy management strategy.

LIST OF ABBREVIATION AND NOMENCLATURE

ABC	Ant bee colony.
Bat	Battery.

The associate editor coordinating the review of this manuscript and approving it for publication was Ahmed Mohamed.

CO_2	Carbon dioxide.
Bio	Biomass.
CS	Cuckoo search.
EL	Electrolyzer.
GA	Genetic algorithm.
GAMS	General algebraic modeling system.
HRES	Hybrid renewable energy system.
LSC-SSA	Levy sine cosine-salp swarm algorithm.
MILP	Mix integer linear programming.
MNLP	Mix non-linear programming.
η_{inv}	Inverter efficiency.
NSGA-II	Non-dominated sorting GA.
N_{HT}	Number of hydrogen tank.
P_{bmg}	Biomass gasifier power.
$P_{inv-out}$	Inverter output power.
P_{bat}^{max}	Maximum battery power.
P_r^{el}	Electrolyzer rating.
P_r^{fc}	Fuel cell rating.
P_r^{ht}	Hydrogen tank rating.
P_r^{pv}	Photovoltaic rating.
P_{pv}	Photovoltaic power.
PSO	Particle swarm optimization.
$P_{storage}$	Power storage.
PV	Photovoltaic.
SoC	State of charge.
SoC_{max}	Maximum state of charge.
SoC_{min}	Minimum state of charge.
T^{noct}	Operating cell temperature.

I. INTRODUCTION

Presently, a substantial barrier impedes the quest for addressing the ever-escalating energy requirements and the associated dilemmas linked with fossil fuel utilization [1]. The call for energy is on an upward trajectory owing to burgeoning economies and a global population surge, consequently driving up the reliance on fossil fuels() [2]. Microgrid has been identified as a sustainable solution for meeting the energy demand [3]. A microgrid is designed to meet the energy demand of a specific area, like a community, campus, or industrial facility, and can function independently or grid-connected [4]. A microgrid powered by renewable energy sources are seen as the most fitting and economical approach for providing an electricity. However, creating the most effective and cost-efficient design for such systems, considering both technical and economic aspects, is a complex task due to various challenges [5]. One of these challenges stems from the unreliability of renewable energy sources, which heavily rely on weather conditions. Frequently, microgrid systems end up being either too large, incurring high costs and producing excess energy, or too small, leading to insufficient power supply for their intended purposes [6]. To address these issues and fully capitalize on the advantages of renewable energy-based microgrids, It is crucial to meticulously establish the optimal size of the microgrid and couple it with a robust energy management strategy [7]. Renewable Energy Resources (RESs) heavily depend on weather conditions, yet they inherently provide advantageous synergies across various times (day and night, as well as different seasons) and spaces [8]. Studies have demonstrated that integrating multiple hybrid RESs offers improved cost-efficiency and dependability compared to a solitary energy system [9]. Recently, there has been a substantial upsurge in the development of environmentally conscious energy technology utilizing fuel cells (FCs). FCs bring forth distinct benefits compared to conventional batteries, attributed to their capacity to produce energy through fuel combustion, a contrast to the simple energy storage mechanism of batteries. This unique attribute positions FC as a remarkably efficient fuel option for generating electricity, owing to their impressive efficiency, considerable power density, and absence of emissions. Operating within an efficiency range of 40% to 60%, fuel cells outshine combustion engines (25%) and power plants by a significant margin [10]. In an effort to enhance the cost efficiency of FC systems, researchers have directed their attention towards diminishing the expense associated with power generation through FCs. Consequently, the cost of power produced by FCs has witnessed substantial reduction over time, declining from $110 per kilowatt (kW) in 2004 to $56.6 per kW in 2012, with anticipations of continued decreases in the future [11]. Identifying an eco-friendly and efficient electricity generation has been a main spotlight for lots of scholars. As one prospective solution, biomass stands out as a promising option due to its ability to generate power without emitting carbon dioxide, making it an efficient and renewable energy source. As a result, the use of biomass for power generation has been gaining more and more interest.

A. PROBLEM STATEMENT

The global energy demand is on the constant statement due to the factors such as population growth, economic growth, urbanization, change in lifestyle etc. This rise in demand is made traditional energy sources such as coal, natural gas, and oil. However, the use of traditional energy sources comes along with a range of challenges like environmental ham, reliability, energy loss in transmission and aging infrastructure. Hybrid renewable energy based microgrid has been endorsed for remote off-grid communities. But designing an optimal microgrid system due to the stochastic resource nature, load variation, and high cost of renewable component. In that line, several optimization algorithms are proposed to optimally design a microgrid system, but the algorithms are prone to

issues like premature convergence, solution trapping in local optima, slow convergence, and low accuracy. Therefore, this paper proposed an improved SSA for the design of optimal HRES. This is motivated by the understanding that even a small improvement in metaheuristic algorithm can lead to a considerable positive influence on the performance of the HRES.

B. LITERATURE REVIEW AND GAPS

Numerous prior investigations have delved into the optimal control and sizing of microgrid that integrate hydrogen fuel cells and battery storage. These studies have employed a diverse array of methodologies and viewpoints. Achieving the most effective arrangement for renewable energy systems usually hinges on leveraging established commercial frameworks and robust meta-heuristic intelligent optimization algorithms. These elements play a pivotal role in attaining optimal outcomes. The ensuing paragraphs delve into a few of these studies.

Table 1 offers a concise overview of a range of research investigations centred around enhancing the design and functioning of microgrid through the integration of hydrogen FC. In reference [12], an examination was carried out involving PV combined with hybrid battery and pump hydro storage. This study harnessed the potential of rainfall under various reliability. The research explored two distinct test bed system: Case-1, which featured a PV integrated with only battery storage, and Case-2, which integrated PV, battery, and pump hydro storage. The investigation encompassed a range of LPSP values, ranging from 0.00 to 0.10 in increments of 0.02. To determine the ideal system size, the optimization process utilized the particle swarm optimization technique, with a primary focus on reducing the LCOE. In [13], researchers introduced an innovative power flow control approach aimed at boosting the efficiency of an energy system. The investigation validated that the interval of start and stop cycles for both an EL and FC is extended by 65% and contracted by 59%, correspondingly. This modification resulted in a significant improvement in the system's ability to produce hydrogen. In [14], researchers employed an improved grey wolf algorithm to derive the optimum size of microgrid system. The study demonstrates that incorporating more than one type of storage as primary backup can mitigates the fluctuations in RES. In reference [15], a grid-connected PV system has been implemented to satisfy the requirements for electrical power, heating, and production of hydrogen. This comprehensive system incorporates electric heaters for centralized solutions in heating and energy storage. The primary objective is to develop and analyze a grid tied system in its initial design phase, conducting an assessment encompassing economic, energy, and environmental aspects. This assessment takes into account critical factors such as the cost of energy (COE), energy rates (ER), and proportion of renewable energy. In [16], an efficient methodology for controlling energy in both isolated and grid-coupled nodes is presented. The study attains a drop in regular operational costs by 1.21%, 0.88% for unrestricted grid operation, and 1.08% for grid operation based on the findings. The system comprises PV, WT, Battery, and an EL. Subsequently, the researchers devised a multi-faceted EMS to control the power consumption of the diverse decentralized energy elements. The EMS's purpose was designed to ensure that both battery storage and the EL operate with a balance of low cost and extended longevity. Reference [17] presents a cost-focused approach designed to discover the most efficient configurations and EMS for an isolated microgrid, leveraging machine learning methods. This framework is built upon two pivotal stages. Firstly, it involves determining the optimum size for of Photovoltaic-Battery Energy Storage system using an analytical and economically oriented sizing model, with a primary objective of minimizing the LCOE. Following this, microgrid's EMS is optimize using machine learning, ultimately leading to the achievement of optimal cost reductions. The research cited as [18] undertook a comparative analysis in the realm of energy storage, comparing hydrogen-based and battery-based solutions. The researchers formulated diverse operational approaches and determined that hydrogen energy storage exhibited superior performance to battery energy storage. This superiority was particularly evident in metrics like financial evaluation, self-reliance metric, and grid performance indicator, especially when faced with instances of grid power fluctuations. In studies [19], researchers examined how the wind power factor and the cost of energy influenced the Cost of Hydrogen (COH). Through the consideration of diverse approaches regarding transportation and hydrogen storage, the results demonstrated that the COH attained its most economical figures, attaining a cost of 7.2 $/kg for production in Argentina and 9.4 $/kg for production in Italy. The research referenced as [20] delved into the advantages of employing combine storage arrangement that integrates hydrogen and battery. The researchers highlighted that battery storage hold a cost advantage, and the incorporation of hydrogen and battery storage offers a promising approach to aaddress the uncertainties associated with renewable energy generation and load variations. As such, hydrogen emerges as a reliable and environmentally pleasant storage solution that harmonizes effectively with battery for energy supply objectives. The research referenced in [21] examined the economics of supplying hydrogen through electrolysis while also reducing the price of supplying hydrogen. The study's model successfully established an optimal configuration for a hybrid system, effectively harnessing resources like wind, solar, and geothermal energy to achieve this ideal setup. The study referenced in [22] utilizes both HOMER and the Performing Platform, an advanced system that integrates optimal dispatch strategies for evaluating plant performance. The investigation encompasses a range of factors, including sensitivity analysis and market circumstances, operational constraints, and the influence of capacity-based incentives. The research outcomes indicate that, under the assumptions they've set, photovoltaic systems combined with battery

TABLE 1. Overview of the literature review.

Ref.	Energy sources of the system					Method	Limitation
	PV	WT	BM	BT	FC		
[23] 2023	✓	✓	✓	✓	×	DE	Reliability not considered. DE converge slowly in high dimensional search spaces.
[24] 2023	✓	✓	×	✓	✓	CSA	CSA can get trapped in local optima, and can converge slowly in high dimensional search spaces.
[25] 2022	✓	✓	×	✓	×	CS, GA, SA, HS, FA.	Reliability not considered.
[26] 2022	✓	✓	×	✓	×	DE	Reliability not considered. Emission not considered.
[27] 2022	✓	✓	×	✓	✓	GA, PSO	Reliability not considered.
[28] 2021	✓	✓	×	✓	×	GWO	Reliability not considered. Single energy storage is considered.
[29] 2021	✓	✓	×	✓	×	SHA	Reliability not considered. Not compared with other Algorithms.
[14] 2021	✓	×	✓	×	✓	WO	Reliability not considered.
[30] 2021	✓	✓	×	✓	×	IGO	Reliability not considered.
[31] 2022	✓	✓	×	✓	×	HSA	The local contribution of the hybrid system in terms of economy and reliability is not further elaborated.
[32] 2022	✓	✓	×	×	✓	NSGA-II	The use of a hysteresis band improves system performance.
[5] 2019	✓	✓	×	✓	×	GO	Emission not considered.
[33] 2023	✓	✓	×	✓	×	DE	Reliability not considered.
[34] 2023	✓	×	×	✓	✓	MILP	Complexity and high computational cost in MILP.
[35] 2023	×	✓	×	×	✓	MNLP	Limited solver availability and derivative information requirement in MINL.
[36] 2018	✓	✓	✓	✓	✓	GA	Reliability not considered. GA suffers from slow convergence problem.
[37]	✓	✓	×	✓	×	IWO	No additional information on the hybrid system and lack of assessment of cost effectiveness of hybrid systems
[38] 2021	✓	✓	×	×	✓	IAEO	Reliability not considered. Lack of justification in peer reviewed articles to explain study
NIL	✓	×	✓	✓	✓	LSC-SSA	Proposed

CSA = cuckoo search algorithm, DE = differential evolution, EL = Electrolyzer, FA = firefly algorithm, HS = harmony search, IWO = improved whale optimization, TRNSYS = transient system simulation, GAMS-MILP = general algebraic modelling system-mixed integer linear programming, GWO = grey wolf optimization, LFA = levy flight algorithm, LSC-SSA = levy sine cosine-salp swarm optimization algorithm, IAEO = improved artificial eco-system optimization, CS = cuckoo search, NSGA-II = non-dominated sorting genetic algorithm II, MILP = mixed integer linear programming, MNLP = mixed integer non-linear programming, ABC-PSO = artificial bee colony-particle swarm optimization, SHA = spotted hyena optimization.

storage configurations generally result in greater profitability. Nevertheless, it's important to highlight that designs incorporating concentrated PV power systems generate substantially higher yearly energy output. Furthermore, concentrated PV power systems equipped with thermal storage, optimized to maximize the ratio of benefits to costs, exhibit a linear relationship that relies on input parameters.

Drawing from the recent works mentioned above, several renewable energy sources were used for the hybrid renewable energy system optimisation. However, the optimal energy management and sizing of photovoltaic-biomass design with hybrid battery-hydrogen energy storage system using LSC-SSA is not reported.

C. CONTRIBUTION AND PAPER ORGANIZATION

The paper proposed an improved SSA for deterministic EMS and capacity optimization that can efficiently control the supply of energy amongst various components of a hybrid system that comprises solar PV, biomass, FC, and battery. Particularly, this approach marks a notable advancement in the field, as it stands as the pioneering method of its kind in the existing literature. The approach considers the limitations and performance characteristics of each element of the system to deliver an effective, dependable, and environmentally friendly power provision.

The contribution of this paper can be summarized as follows:

- The incorporation of rule-based supervisory EMS and LSC-SSA to enhance the efficiency and effectiveness of the EMS and sizing of the proposed microgrid.
- To demonstrate the superior performance of EMS-LSC-SSA by comparing its results with those obtained from EMS-SSA and EMS-GA.
- Assess the optimum values of the decision variables relating to the system components, which comprise the solar PV, Biomass, number of hydrogen tank (N_{HT}), and battery.

This paper is organized in the following manner. Section II provides the system testbed and mathematical model of the proposed HRES components. Section III presents the objective function. Section IV discusses the levy sine cosine-salp swarm algorithm. Section V presents the results and discussion. Finally, the extracted conclusions are summarized in Section VI.

II. MATERIALS AND METHOD

This section presents the methodology of the research. The main goal of the research is to design a grid independent HRES and integrates solar, biomass, FC, and battery that will supply the energy requirement of an isolated households. Figure 1 depict the representation of the microgrid. To balance the unstable energy production from the intermittent resources such as solar, a hydrogen FC and battery are integrated to the microgrid. The FC comprises of an EL, and H_2 storage. The following section provides an overview of the mathematical models for each component and the supervisory EMS for the hybrid RES.

A. SOLAR PHOTOVOLTAIC MODEL

Solar power generation is determined by temperature and sunlight intensity. The energy produced per solar PV panel unit can be computed using (1) [39], expressed as:

$$P_{pv\_out} = P_{N\_PV} \times \frac{G}{G_{ref}} \left[1 + K_t \left((T_{amb} + (0.0256 \times G)) - T_{ref}\right)\right] \quad (1)$$

where, P_{pv_out} is the PV output power, P_{N_PV} refers to power under reference condition G_{ref}, G is the insolation (W/m^2),

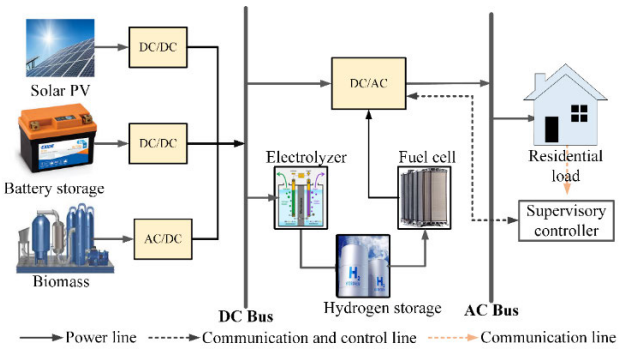

FIGURE 1. Schematic diagram of the proposed hybrid system.

TABLE 2. Technical parameters of the renewable components [39].

Components	Parameters	Values	Unit
Photovoltaic module	P_r^{pv} at STC	1	kW
	T^{noct}	48±2	^{0}C
	η_{pv}	16.9	%
Biomass	P_r^{bmg}	4	kW
	CV_{bmg}	18	MJ/kg
	η_{bmg}	21	%
Electrolyser	P_r^{ele}	1	kW
	η_{ele}	75	%
Hydrogen tank	P_r^{ht}	1	kg
	Heating value	39.72	kWh/kg
Fuel cell	P_r^{fc}	1	kW
	η_{fc}	40	%
Battery	$B_{cap.}$	45.2	kWh
	η_{bat}	0.85	%

P_r^{pv}= photovoltaic rating, T^{noct} = nominal operating cell temperature, η_{pv} = photovoltaic efficiency, P_r^{bmg} = Biomass gasifier power, CV_{bmg} = biomass caloric value, η_{bmg} = biomass efficiency, P_r^{ele} = Electrolyzer rating, η_{ele} = electrolyzer efficiency, P_r^{ht} = Hydrogen tank rating, P_r^{fc} = Fuel cell rating, η_{fc} = fuel cell efficiency, $B_{cap.}$ = battery capacity, η_{bat} = battery efficiency.

K_t is $-3.7 * 10^{-3}(1/0C)$, T_{ref} is 25^{0}C and T_{amb} represent temperature. The nominal description of the solar PV is specified in Table 2.

B. BIOMASS MODEL

The annual energy production (E_{bm}) from biomass can be determined by applying (2) [40], expressed as:

$$E_{bm} = P_{bm} \times (8760 \times CUF) \quad (2)$$

where P_{bm} stand for the rating of the biomass system and CUF refers to capacity utilization factor. The efficiency of bio-based system relies on various variables, encompassing the energy content of the biomass, the annual biomass quantity accessible (measured in tons), and duration of biomass utilization. Despite biomass being bulky devices prone to operational interruptions, these difficulties can be tackled by incorporating storage systems like hydrogen and battery. These storage solutions aid in mitigating disruptions to the

system and counteracting energy imbalances arising from gasifier interruptions. Additionally, ensuring uninterrupted operation during outages can be achieved by setting up duplicate biomass gasifiers or incorporating backup energy sources. By employing (3) [9], one can calculate the highest capacity of a biomass suitable for a given location:

$$P_{bm} = TBA(Ton/yr) \times 1000 \times CV_{bm} \times \eta_{bm}/ 365 \times 860 \times hr/day \quad (3)$$

The conversion efficiency is denoted by η_{bm}, CV_{bm} denote the calorific value of the given biomass being used and TBA stands for total biomass available [39]. The nominal description of the biomass is presented in Table 2.

C. EL, H_2 AND FC MODEL

The transfer of energy from the EL to the H_2 tanks is denoted by the expression in (4) [41].

$$P_{el-ht} = P_{ren-el} \times \eta_{el} \quad (4)$$

where P_{el-ht} represent the ultimate power from the EL, P_{ren-el} is the power supplied to the EL using renewable energy, and η_{el} is the of the efficiency EL.

The effectiveness of an EL is estimated by taking the ratio of the output power (P_{el-ht}) to the input power (P_{ren-el}).

The subsequent equations represent the stored energy level of the H_2 storage at each time point t, as H_2 is electrolyzed from the EL and stored under pressure [38].

$$E_{ht}(t) = E_{ht}(t-1) + P_{ren-el}(t) \times \Delta t - P_{ht-fc}(t) \times \Delta t \times \eta_{ht} \quad (5)$$

$$M_{ht}(t) = E_{ht}(t)/HHV_{H_2} \quad (6)$$

where $E_{ht}(t)$ and $E_{ht}(t-1)$ stand for the energy contained within the H_2 tank at both time t and time $t-1$, P_{ht-fc} denotes the power supplied into the FC from the H_2 tank at the time t, η_{ht} represents the efficiency of the H_2 tank, and Δt denotes the time interval, set at 1 hour. In addition, $M_{ht}(t)$ signifies the quantity of hydrogen introduced into the H_2 tank, while HHV_{H_2} denotes the high heating value of H_2, standing at 39.72 kWh/kg.

Proton exchange membrane FCs are commonly utilized for power generation in various applications, including automobiles and portable electricity generation units [42]. FC exhibit a power generation efficiency typically ranging between 40-60%, which surpasses many alternative methods of energy conversion. The energy generated by FCs is considered to be around 40%, which is characterized by (7) [9] as:

$$P_{fc-inv} = P_{ht-fc} \times \eta_{fc} \quad (7)$$

where η_{fc} represent the FC efficiency.

The parameters of the EL, H_2 storage and FC are provided in Table 2.

D. MODEL FOR BATTERY STORAGE

A lithium battery is used in this research because of its greater effectiveness and the major drop in price, as mentioned in [43]. The C_{rate}, which represents the maximum charge and discharge capability of a battery, is a crucial factor in battery modeling as it governs the flow of energy between renewable sources, the battery, and the energy demand, principally when it comes to charging and discharging the battery. The solar PV are erratic and may possibly produce more or less power than required. Equation (8) [44] illustrates whether the battery is receiving or supplying power based on the surplus or deficit in power generation.

$$P_B(t) = (P_{PV}(t) + P_{WT}(t)) - P_L(t)/\eta_{inv} \quad (8)$$

The symbol n_{inv} represents the efficiency of an inverter. If $P_B(t) > 0$, it signifies that the solar PV generates excess power than needed, whereas $P_B(t) < 0$ indicates an insufficient power generation. The battery can only be charged when there is surplus power generation or when the State of Charge (SoC) falls below the maximum SoC (SoC_{max}), Similarly, (9) represents the SoC of the battery during charging at time t [45].

$$SoC(t) = SoC(t-1)(1-\sigma) + ((P_{PV}(t) + P_{WT}(t)) - P_L(t)/\eta_{inv}) \times n_B \quad (9)$$

where σ stand for hourly self-discharge rate of the battery and n_B denotes the efficiency of the battery.

When PV generation is inadequate and the battery is beyond the acceptable limit, SoC (i.e., $SoC(t) < SoC_{min}$), the battery discharges to meet requirement according to (10).

$$SoC(t) = SoC(t-1)(1-\sigma) - (P_L(t)/\eta_{inv} - (P_{PV}(t) + P_{WT}(t))) \times n_B \quad (10)$$

The subsequent formulation estimates the storage capacity of the battery according to the chosen self-sufficiency day and the requirement as in (11) [46].

$$B_{cap} = AD.E_L/\eta_{inv} \times \eta_B \times DoD \times V_S \quad (11)$$

E. INVERTER MODEL

The modeling of an inverter connecting the loads to the microgrid system relies on its efficiency (η_{inv}). The selected inverter must have the capability to handle the maximum anticipated loads and any potential power surges when appliances are initially powered on. The study takes into account an inverter with an efficiency rating of 92%. The output power of the inverter is given by (12) [39]:

$$P_{inv,out} = (P_{pv} + P_{wt} + P_{bmg} + P_{storage}) \times \eta_{inv} \quad (12)$$

F. SUPERVISORY ENERGY MANAGEMENT STRATEGY

An effective EMS is essential for ensuring a reliable microgrid system. In this study, biomass is regarded as the least preferred option, utilized only when the PV, FC, and battery systems are unable to fulfill the energy demand. The

operational approach of the system can be summarized in the following sequence.

- When the PV power output matches the load demand, that is $P_{pv}(t) = P_L(t)$, In this case, the PV power is sufficient to fulfill the load demand.
- If the PV power generation exceeds the load demand, indicated by $P_{pv}(t) > P_L(t)$, any surplus power from both solar and wind sources can be stored in the battery bank, as long as the SoC is below its maximum capacity $SoC(t) < SoC_{max}$.

The symbol 'P_L' represents the instantaneous demand requirement.

- If the stored energy in the battery $P_{bat}(t)$ surpasses the upper limit $P_{bat}^{max}(t)$ in the aforementioned situation, the excess energy is supplied to the EL.
- If the PV is not producing sufficient power, that is $P_{pv}(t) < P_L(t)$, the deficit can be offset by the battery.
- When the power produced by the PV cannot meet the load demand, and the energy stored in the battery is also inadequate to supply the load requirement, then the combined energy from the battery and FC can be utilized to supply the deficit demand.
- If PV supply cannot meet the load demand, and the combined batteries and FC are unable to supply adequate power to fulfil the load requirement, the load can be met through the utilization of a biomass.

Fig. 2 represents a streamlined flow chart that explains the operating scheme of the proposed EMS of the microgrid.

III. CASE STUDY

Nigeria, a vast nation covering 923,768 square kilometres, shares borders with Chad and Cameroon to the east, Benin to the west, and Niger to the north. While cities and towns are linked to either the national or isolated power grid, villages and settlements located in remote areas rely on diesel generators to power their electricity needs. However, it is challenging to ensure a consistent supply of fuel and electricity due to factors such as difficult road conditions during the rainy season, periodic maintenance shutdowns of gas plants, and the high cost of fuel. This research considered a rural village in Borno State, situated in the northeast region of Nigeria to test the practicality and efficiency of a microgrid concept and capacity planning strategy. The precise location of the village being studied can be found in Figure 3.5. The study site encompasses an expanse of 2572.345 square kilometres and is situated at latitude 12.508837 N and longitude 13.104142 E. This region is abundant in natural resources, particularly solar energy. Furthermore, the potential of biomass energy is high as farmers predominate in the chosen location, so agricultural waste products (such as rice husk, maize stover, etc.) can be use as the gasifier's feedstock. These materials are abundant and comprise of the inedible portions of plants that are typically discarded and left to decompose on farmlands.

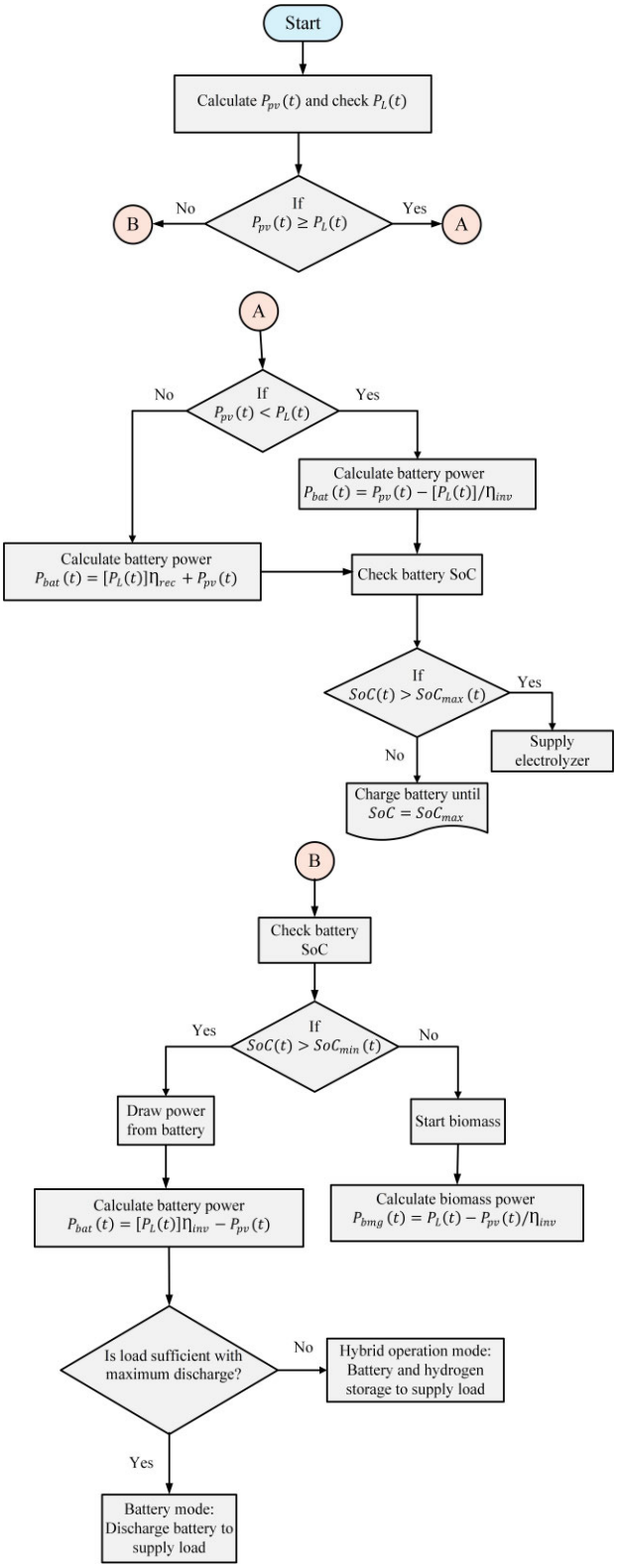

FIGURE 2. Simplified flow chart of the proposed hybrid energy system.

IV. OBJECTIVE FUNCTION

The primary goal of the study is to reduce the overall ASC of the hybrid system under consideration, all while ensuring

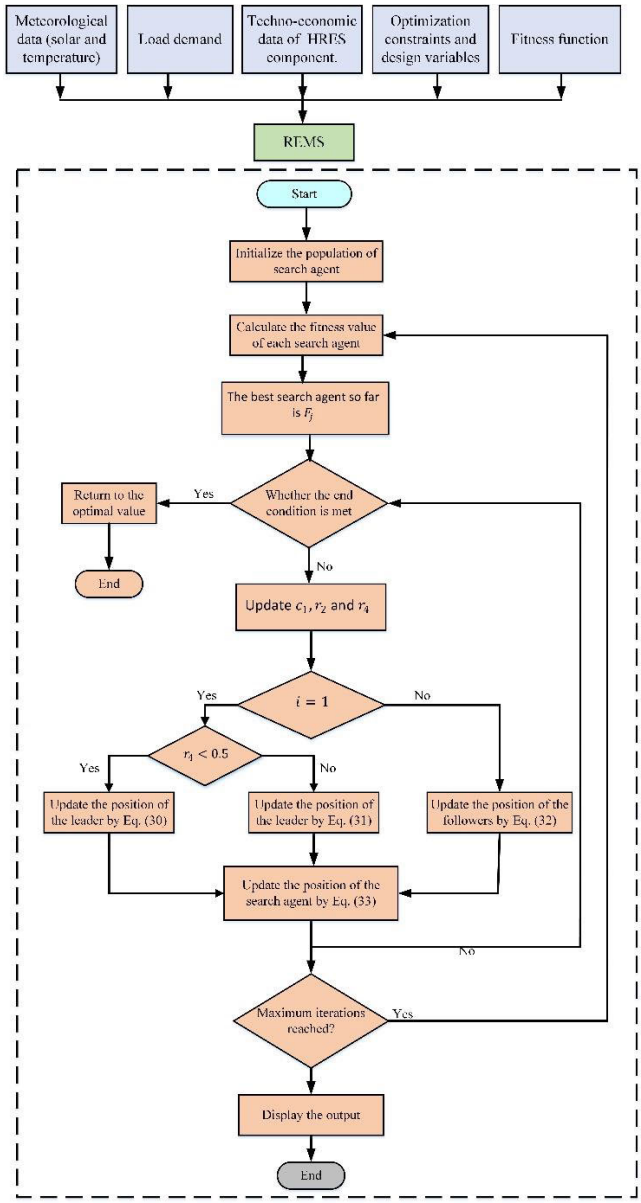

FIGURE 3. Flow chart of the proposed method.

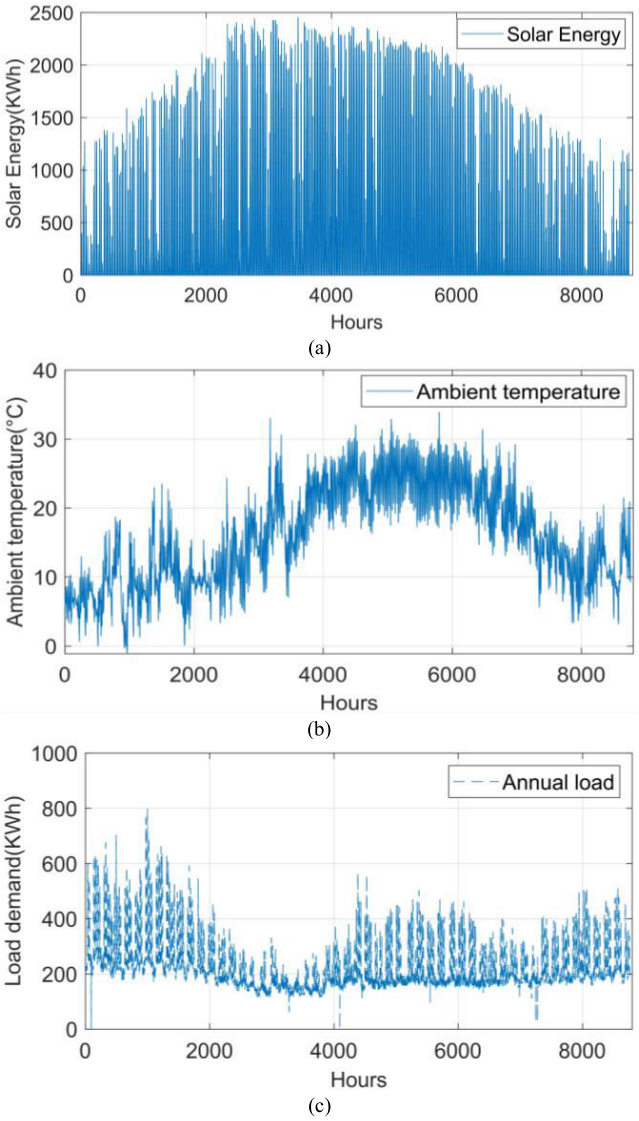

FIGURE 4. (a) Annual Solar radiation (kW/m2), (b) Ambient temperature (A°C), and (c) Load profile (kWh).

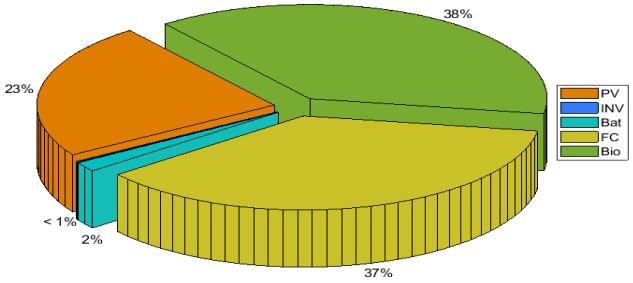

FIGURE 5. Breakdown of the total ASC for the optimal HRES configuration.

an efficient distribution of energy. To achieve the best possible setup, four key factors were identified for decision-making: sizing of PV panels, batteries, and hydrogen FC. The evaluation of the cost of system over a year is employed for economic assessment. Among solutions that meet all limitations and variables, the one with the lowest ASC is determined as the most favourable. The objectives to minimize encompass the annualized system cost, reflecting the financial angle, and the loss of power supply probability (LPSP), reflecting the technical perspective.

A. ECONOMIC ANALYSIS

The ASC stands out as a prominent indicator utilized to assess the financial viability of a standalone microgrid. The equation denoted as number (13) represents the central goal that needs to be minimized, all while taking into consideration the various limitations.

$$ASC(\$/kWh) = F(N_{sol}C_{sol} + N_{bat}C_{bat} + N_{el}C_{el} + N_{ht}C_{ht} + P_{fc}C_{fc} + P_{bm}C_{bm} + P_{inv}C_{inv}) \quad (13)$$

where the costs for PV panels, biomass, EL, H_2 tank, FC, batteries, and inverters are given as C_{sol}, C_{bm}, C_{el}, C_{ht}, C_{fc}, C_{bat}, and C_{inv} respectively. N_{sol}, N_{bat}, N_{el}, and N_{ht} denote the number of PV, battery, EL, and H_2 tank. The capacities of biomass system, FC and inverter are denoted as P_{bm}, P_{fc}, and P_{inv} in that order.

The ASC for the installed system comprises various elements, such as the initial capital and installation cost C_{cap}, replacement cost C_{rep}, annual maintenance cost $C_{o\&m}$, and salvage cost C_s. The total ASC for each component can be expressed as follows:

$$C_{sol} = C_{sol}^{cap} + C_{sol}^{rep} + C_{sol}^{o\&m} - C_{sol}^{sal} \quad (14)$$
$$C_{bat} = C_{bat}^{cap} + C_{bat}^{rep} + C_{bat}^{o\&m} - C_{bat}^{sal} \quad (15)$$
$$C_{el} = C_{el}^{cap} + C_{el}^{rep} + C_{el}^{o\&m} - C_{el}^{sal} \quad (16)$$
$$C_{ht} = C_{ht}^{cap} + C_{ht}^{rep} + C_{ht}^{o\&m} - C_{ht}^{sal} \quad (17)$$
$$C_{fc} = C_{fc}^{cap} + C_{fc}^{rep} + C_{fc}^{o\&m} - C_{fc}^{sal} \quad (18)$$
$$C_{bm} = C_{bm}^{cap} + C_{bm}^{rep} + C_{bm}^{o\&m} - C_{bm}^{sal} \quad (19)$$
$$C_{inv} = C_{inv}^{cap} + C_{inv}^{rep} + C_{inv}^{o\&m} - C_{inv}^{sal} \quad (20)$$

The annualized cost of any system can be determined using the Capital Recovery Factor (CRF), which is employed to calculate the present value of money and can be mathematically represented as follows:

$$CRF(i, N) = i(i+1)^N \Big/ (i+1)^N - 1 \quad (21)$$

Here, N represents the total number of years in the system's lifetime, and i denotes the annual interest rate. The assessment of LCOE and reliability aids in determining the optimal configuration. The LCOE of the system, which is a measure of the average cost per kWh of the energy generated by the system, can be mathematically expressed as:

$$LCOE = ASC(\$/year) \Big/ Total\ useful\ energy\ served(kWh/year) \quad (22)$$

B. RELIABILITY ASSESSMENT

In the process of developing a HRES, ensuring reliability becomes an essential consideration. Within the existing literature, numerous measures of reliability are introduced. Some of the most commonly utilized metrics for evaluating the dependability of any given system comprise the loss of power supply probability (LPSP), projected energy loss, loss of load hours (LOLH), and the comparable loss factor. In this research, the reliability of the standalone microgrid is measured by LPSP. The name 'Loss of Power Supply Probability' refers to the likelihood of not being able to meet the total load demand because of insufficient electricity production capability. This probability is determined by the ratio of total Loss of Power Supply (LPS) to the overall load demand in a given time. LPS is calculated based on the difference between power generation, capacity of storage, and the real energy demand, using the following formula:

$$LPSP = \sum LPS \Big/ \sum P_{Load} \quad (23)$$

V. LEVY SINE COSINE-SALP SWARM ALGORITHM

The Salp Swarm Algorithm (SSA) is a form of swarm intelligence optimization strategy designed to replicate the collective movement of salp organisms in an interconnected manner within oceanic environments. Acknowledging the limitations inherent in SSA, such as suboptimal precision, constrained optimization when dealing with lower dimensions, and gradual convergence, an improved iteration named the Enhanced Salp Swarm Algorithm has been introduced. This enhanced version, referred to as (LSC-SSA), integrates the characteristics of Levy flight and the sine cosine operator. The Levy flight element encompasses a blend of short steps and long leaps to navigate the solution space, significantly boosting the algorithm's capability to explore a wide global spectrum. Meanwhile, the sine cosine operator employs a sine-based search for extensive global exploration, while the cosine-based search is employed to exploit local regions more effectively.

The mathematical equation representing the Levy operator for updating the salp swarm's position is detailed as follows.

$$X_j^i = X_j^i + a.S\Phi X_j^i \quad (24)$$

Within the context of the salp swarm algorithm, the leader's role involves directing the followers, enabling the entire population to adjust its movement based on the food's location. To put it differently, modifying the leader's position alone facilitates a cascading movement throughout the salp swarm. The approach for updating the leader's position in the SSA algorithm employs the population update mechanism outlined in the sine cosine algorithm. The equations governing the adjustment of the leader's position using the sine cosine operator are outlined as follows.

$$X_j^1 = X_j^1 + c_1.\sin(r_2).\left|F_j - X_j^1\right|.e^1 \quad (25)$$
$$X_j^1 = X_j^1 + c_1.\cos(r_2).\left|F_j - X_j^1\right|.e^1 \quad (26)$$

The method for updating the position as presented in Equation (25) can utilize the sine function to facilitate global exploration, while (26) can employ the cosine function to enhance local exploitation. The parameter c_1 allows the search agent to dynamically switch between the two search modes during optimization, facilitating a smooth transition between exploration and exploitation. In its role as a global convergence factor, parameter c_1 contributes to the algorithm's convergence as the number of iterations increases. Upon introducing the global convergence factor c_1 and parameter r_4, a hybrid approach combining both search methods can be employed. The equation is detailed as follows:

$$X_j^1 = X_j^1 + c_1.\sin(r_2).\left|F_j - X_j^1\right|.e^1 if r_4 < 0.5 \quad (27)$$
$$X_j^1 = X_j^1 + c_1.\cos(r_2).\left|F_j - X_j^1\right|.e^1 if r_4 \geq 0.5 \quad (28)$$

TABLE 3. Statistic result for benchmark methods.

Function	LF-SSA		SSA		GA	
	StD	Mean	StD	Mean	StD	Mean
F_1	0.012	0	0.018	8.8E-09	0.023	0.497
F_2	-3.191	-2.991	-3.140	-3.1201	-3.131	-3.131
F_3	-3.862	2.9E-01	-3.862	-7429.82	-3.200	0.970
F_4	-1.920	-1.920	-1.800	-1.791	-1.700	-1.700

Optimization algorithms are commonly evaluated using benchmark test functions to assess their accuracy, time efficiency, and optimality. In this study, the performance of the proposed LSC-SSA algorithm, as well as two other algorithms (SSA and GA), is analysed and compared. The results, including mean and standard deviation values, are presented in Table 3, which serves as a reference for benchmarked outcomes. These algorithms were chosen due to their widespread applicability for various purposes. Four popular benchmark test functions (Sphere, Schwefel, Ackley, and Weierstrass) were mathematically defined. These functions were implemented to quantitatively measure the performance of the nature-inspired metaheuristic algorithms used in this study. The simulation was performed over 100 iterations, and the results were collected for each algorithm, running each 30 times. The best solution's mean and standard deviation values were computed to facilitate a comprehensive comparison of the overall performance of the utilized algorithms, as detailed in Table 3.

The methodology for employing the LSC-SSA to solve the given problem is given as follows:

Step 1: Input Data:

- Meteorological data, including solar irradiation and ambient temperature, from the designated database.
- Load requirements from the load requirement database.
- Techno-economic specifications of the microgrid components, as outlined in Table 2.
- Economic statistics data, encompassing project lifecycle, interest rate, and inflation, as described in Table 2.

Step 2: Initialize the parameters for the LSC-SSA algorithm as follows:

- Population size (n) is set to 40.
- The number of iterations (T) is set to 100.
- The step size control factor (a) is set to 0.01.

a) Set constraints:

- LPSP as; $0.001 \leq LPSP \leq 0.1$

b) Set the search space:

$$1 \leq N_{pv} \leq N_{pv}^{max}; 1000 \leq N_{pv} \leq 3000$$

$$1 \leq N_{bat} \leq N_{bat}^{max}; 200 \leq N_{bat} \leq 1000$$

$$1 \leq N_{ht} \leq N_{ht}^{max}; 100 \leq N_{ht} \leq 250$$

Step 3: Evaluate Search Solutions:

- Calculate the fitness value for each search agent and identify the one with the best fitness value in the current population as the 'food' F_j.

Step 4: Adjust the value of c_1 using (29) and generate random numbers r_2 and r_4.

$$c_1 = 2e^{-(4t/T)^2} \tag{29}$$

When $i = 1$, update the leader's position using (30) and (31). If $i \geq 1$, update the follower's position according to (32). $t = t + 1$.

$$X_j^1 = X_j^1 + c_1 . \sin(r_2) . \left| F_j - X_j^1 \right| .e^1 if r_4 < 0.5 \tag{30}$$

$$X_j^1 = X_j^1 + c_1 . \cos(r_2) . \left| F_j - X_j^1 \right| .e^1 if r_4 \geq 0.5 \tag{31}$$

$$X_j^i = 0.5(X_j^i + X_j^{i-1}) \tag{32}$$

Step 6: Modify the position of the salp swarm using a Levy flight approach, as defined in (33). $t = t + 1$

$$X_j^i = X_j^i + a.S\Phi X_j^i \tag{33}$$

Step 7: Check if the algorithm has reached either the maximum permissible iterations or has discovered the optimal solution. If the algorithm's termination criteria are satisfied, provide the best possible value, and conclude the process. If not, move forward to Step 3. Figure 3 depicts the flowchart of the rule-based levy-sine-cosine salp swarm algorithm (RSC-LSC-SSA), utilized for solving standalone HRES planning problem. The LSC-SSA algorithm adheres to the following steps as indicated.

VI. RESULTS AND DISCUSSION

The research introduced an approach employed to design a Renewable Energy Microgrid (REM) that incorporates solar power, biomass, FC, and battery, as shown in Figure 1. The REM is proposed to meet the load demand of an off-grid community located in northeastern Nigeria. The chosen location benefits from abundant and reliable solar resources throughout the year. Figure 4 gives insights into the load models, solar radiation, and ambient temperature data that were considered for this study. The site also had an abundant supply of biomass material, making it suitable for the setting up of a biomass. The cost of biomass, which includes expenses related to transportation, storage, and labor, was stated to be $25 per ton [39]. In this study, a project duration of 20 years and an assumed interest rate of 6% were employed.

The configurations for the SSA and GA algorithms used in this study is given in Table 4. The implementation of the proposed algorithm and its counterparts is conducted using MATLAB R2021a on an Intel® Core™i5-8250U Processor with 6MB cache, capable of reaching speeds up to 3.40 GHz.

A. OPTIMAL SIZING AND OPERATIONAL STRATEGY RESULTS

The research aims to identify the best configuration for a hybrid energy system incorporating solar PV, biomass, FC, and battery storage. The optimization aimed to achieve minimum levelized cost of electricity (LCOE) while ensuring a reliable and resilient power supply. The three optimization algorithms used in this study were: LSC-SSA, SSA, and GA. The optimization process considered several parameters,

TABLE 4. The parameters settings of ssa and ga algorithms.

SSA Algorithm	GA Algorithm
Population $n = 40$	Population Size $n = 40$
Number of iterations $T = 100$	Number of iterations $T = 100$
Step size control factor= 0.01	Distribution index for crossover: 20
	Distribution index for mutation: 20
	Crossover probability: 0.8
	Mutation probability: 0.2

TABLE 5. Results of the optimization algorithms.

Algorithm	PV (kW)	Biomass (kW)	Battery (kWh)	N_{HT}	LCOE ($)	LPSP (%)
LSC-SSA	2374	2652	461	203	0.927321	0.04
SSA	2385	2648	482	202	0.930552	0.05
GA	2435	2655	476	208	0.948750	0.04

including the capacity of the PV array, biomass, battery storage, number of H_2 tank, loss of power supply probability (LPSP), and annual system cost (ASC). Table 5 represent the optimization result of study. The three algorithms provide similar results in terms of PV array, biomass, and battery capacities. GA suggests a slightly higher PV array capacity, while SSA suggests a slightly larger battery capacity. However, the differences in capacities among the algorithms are relatively small. N_{HT} values are also quite similar among the algorithms, with GA suggesting a slightly higher value. This indicates that the algorithms agree on the required N_{HT} level for the system.

The LCOE values for LSC-SSA, SSA, and GA are close, but LSC-SSA offers the lowest LCOE, indicating that it provides the most cost-effective solution among the three algorithms. LSC-SSA and GA both suggest a 0.04% LPSP, while SSA suggests a slightly higher value of 0.05%. The ASC is the highest for GA and the lowest for LSC-SSA. This aligns with the LCOE results, as a lower LCOE generally leads to ASC. LSC-SSA produces the most cost-efficient design in terms of annual cost.

Figure 5 provides a detailed breakdown of the total ASC attributed to various components of the HRES. As depicted in the figure, the solar PV, Bio, FC, INV, and Bat components contribute 23%, negligible, 38%, 37%, negligible, and 2%, respectively, to the overall ASC. It's worth highlighting that the FC and Bio elements, serving as the primary and secondary backup power sources, represent the most substantial portions of the total ASC.

B. ANALYSIS OF POWER GENERATION

Figures 6 and 7 depict the monthly outputs of each component within the optimized REM, and the percentage of energy generated by each source, as determined through the LSC-SSA optimization. As demonstrated in Figure 6, the monthly mean solar PV generation put on display of a different recurring pattern that aligns with the solar radiation, with

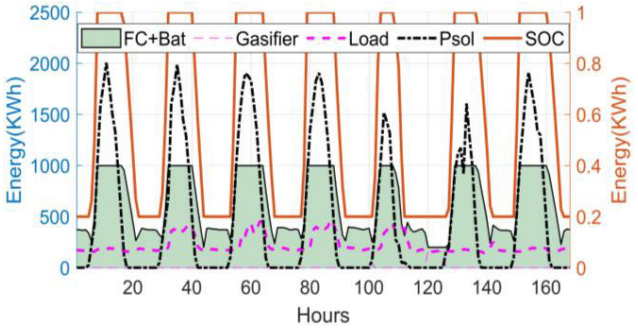

FIGURE 6. Energy output of each component in the HRES.

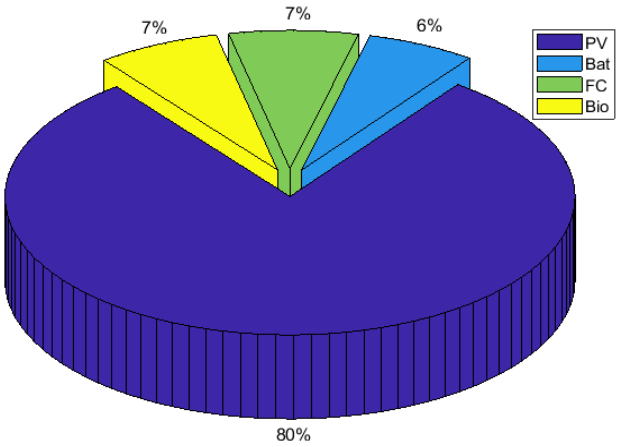

FIGURE 7. The proportion of energy generated by the energy source within the proposed HRES.

the maximum generation observed in the month of July and a gradual decline from August to December. Power generation from biomass follows solar PV power generation, with its peak output occurring in January. FC generation mirrors the trend of solar PV power generation, responding to seasonal variations. Biomass generation is the next source in line after PV generation. It serves as a backup option whenever the primary supply, consisting of PV and the two backups, FC, and battery, falls short of meeting the load demand. As illustrated in Figure 7, the energy generation distribution within the REM showcases the significant contribution of the solar PV, accounting for 80% of the total energy generated. In contrast, the Bio, FC, and Bat systems individually make up smaller proportions of the generated energy, with shares of less than 7%, 7%, and 6% respectively.

C. ANALYSIS OF SUPERVISORY EMS

Figures 8 provide graphical interpretations of the energy balance between energy supply and demand across the Winter, Spring, Summer, and Autumn seasons, respectively.

In Winter season, as depicted in Figure 8, it becomes evident that the renewable energy generated falls short of

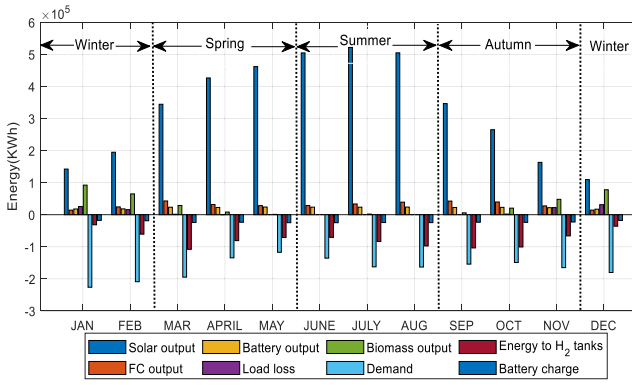

FIGURE 8. Monthly energy balance average over a year.

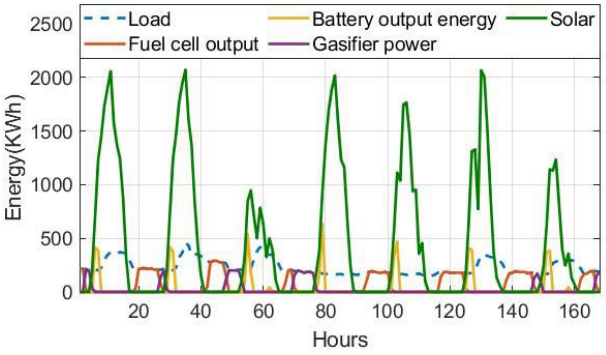

FIGURE 9. Hourly generation for a week of the year caption.

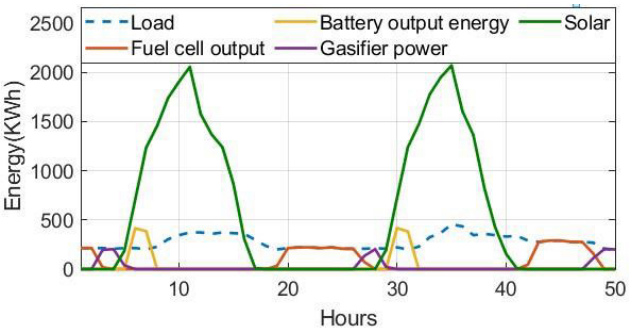

FIGURE 10. Hourly generation within the first 48 hours of the week.

meeting the energy demand. Furthermore, the energy of the FC and battery storage system is insufficient to cover the load requirements. To compensate for the energy shortfall, biomass is strategically employed in accordance with the operational plan.

Transitioning to the Spring season, refer to Fig 8, a significant increase in power generation from solar PV is witnessed due to good solar radiation, implying constant climatic conditions without significant cloud coverage. Notwithstanding this boost in solar generation, the energy generated remains insufficient to satisfy the load demand. Additionally, the energy supplied by the FC and battery cannot bridge the energy gap, even with the augmented FC output. To take care of the energy shortfall, biomass comes into play to ensure load requirements are met during the Spring season. In the Summer season, solar PV generate the highest amount of energy, mainly due to abundant solar radiation. Particularly from June to August, the energy generation is more than adequate to meet the load demand. The surplus energy generated is utilized for charging the battery storage system and powering the electrolyzer for hydrogen production. Consequently, there is no need for biomass power generation during the Summer season. As for the Autumn season, refer to Figure 8, a decline in power generation from September to November is witnessed. This decrease is primarily attributed to reduced solar radiation and increased fog experience in the season. Subsequently, energy from biomass, FC, and battery storage progressively raises as the season advances from its onset to its conclusion.

Figure 9 illustrates a detailed representation of how power is distributed among the various sources throughout a one-week span. Its primary aim is to offer a lucid comprehension of how power flows between these energy source. As previously discussed in the operational approach, when the solar PV fail to produce adequate electricity, and the combined capacity of the FC and battery falls short of meeting the required load, the system turns to a biomass for support. The diagram highlights instances when solar PV energy output is notably low, prompting the activation of the biomass gasifier to supply power during those specific hours.

Figure 10 offers a thorough hour-by-hour examination of energy generation and the sources during the first 48 hours of the week considered in Figure 8. It underscores the fluctuations in energy generation and the corresponding operational methods for different time periods. In Figure 9, during the time frame spanning from 00:00 h to 04:00 h, the solar PV is inactive in generating power. This is primarily attributed to overcast weather conditions during the winter months. To compensate for the absence of power generation from solar PV sources, the energy requirement is satisfied by FC from 00:00 h to 02:00 h, and biomass from 02:00 h to 04:00 h. Furthermore, between 04:00 h and 17:30 h, the power generated by the solar PV is more than the load demand. The surplus is used to charge battery and supply EL for hydrogen production. From 17:30 h to 26:00 h, the solar PV is once again inactive, and the load requirement is exclusively met by the FC. The same pattern of power generation is repeated for the remaining hours.

Figures 11 and 12 demonstrates the dynamic integration of energy sources and the resulting electrolyzer output over a week in the summer season. The abundant presence of solar PV eliminates the need for biomass energy during this period. For a more detailed breakdown of the initial 48 hours of the summer season, refer to Figure 12. Between 0h and 5h, the load is supplied with a diverse mix of energy sources, including solar PV, combined with fuel cell and

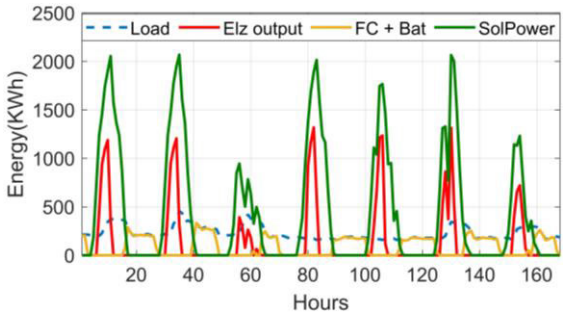

FIGURE 11. Weekly output generation with corresponding EL production.

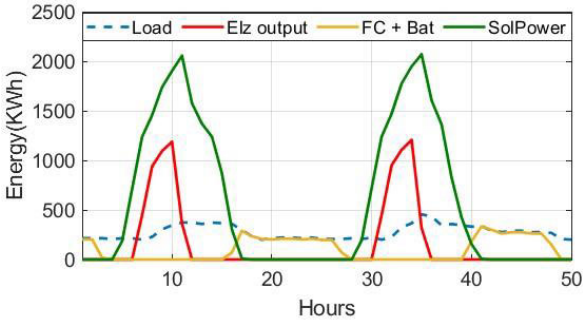

FIGURE 12. Hourly generation in first 48 hours with corresponding EL production.

battery power. Subsequently, from 5h to 15h, the load is predominantly supported by solar PV power. Any surplus solar energy generated during this time is efficiently directed to the electrolyzer for hydrogen production in accordance with the operational strategy. The electrolyzer commences its operation at 6h and continues until 12h, coinciding with the period of peak solar generation. Between 17h to 28h, the load is met with a combination of FC and battery power. From 28h to 41h, the load is fulfilled by the joint resources of solar with combined FC and battery. Notably, the electrolyzer's production output initiates at 30h and concludes at 36h, aligning with the period of high PV output. From 41h to 48h, the load demand is met using FC and battery as the primary energy sources.

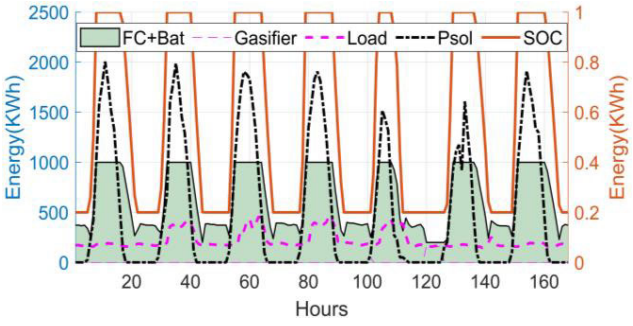

FIGURE 13. Energy generation mix versus combined FC and battery output for a week.

Figure 13 presents a comprehensive depiction of the entire power generation by solar PV and biomass versus the combine power from FC and battery storage taking place over the course of a seven-day duration. On the left-hand side of the chart, a vertical axis displaying solar PV power, biomass power, combined FC, and battery power. The corresponding state of charge (SoC) for the battery is also indicated on the right side of the diagram.

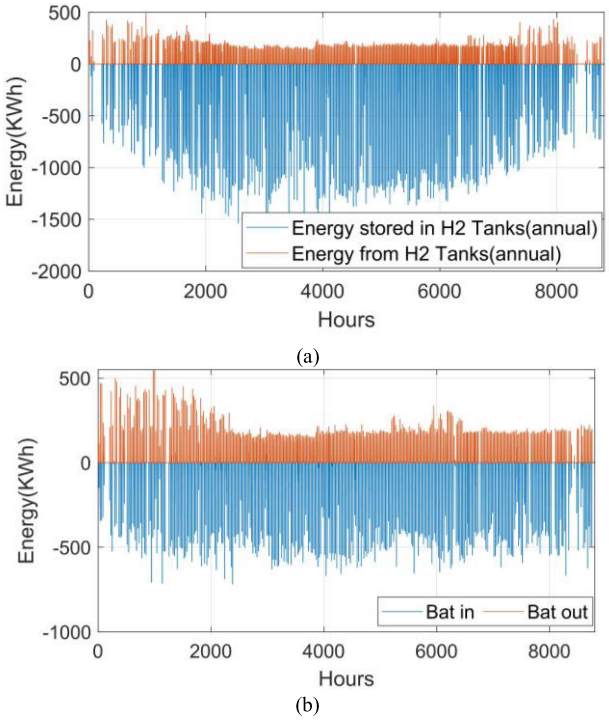

FIGURE 14. Annual energy input and output for (a) Hydrogen (b) Battery.

In setups where hydrogen and batteries are employed for storage, it is crucial to consider the energy inflow and outflow of these elements. Figure 14 offers a graphical depiction of the energy dynamics for both hydrogen and battery storage over the course of a year. The figure illustrates that, in general, both components receive and supply an adequate amount of energy. Nevertheless, it is of utmost importance to consistently monitor the charging and discharging rates of the battery.

VII. CONCLUSION

This paper suggests incorporating a hybrid approach, which combines the LSC-SSA with rule-based supervisory EMS and sizing. Integrating multiple renewable energy sources into a unified energy system enhances reliability, cost-effectiveness, and adaptability, particularly in off-grid or remote areas. The main objective is to secure a continuous and dependable annual power supply to an isolated rural site situated in North-eastern Nigeria, covering the expected 20-year operational span of the system. To strengthen energy source management, the REM integrates conventional

battery energy storage. This integration aims to enhance the system's design, reducing the overall ASC over its lifespan. Furthermore, a key aim is to guarantee a high level of reliability, with a maximum allowable limit of 0.001 to 0.1 LPSP. To attain this goal, the LSC-SSA Algorithm is employed to identify the most optimal configuration for the REM. The optimization performance of the algorithm is evaluated against two other algorithms to showcase the efficiency of the proposed method.

The findings yield the following conclusions: The combination of solar PV, biomass, and fuel cell (FC) energy sources demonstrates substantial potential as an alternative design for a Renewable Energy Microgrid (REM). This hybrid approach allows for diversified and sustainable energy generation.

The LSC-SSA method exhibits superior convergence and resilience in achieving optimal sizing for the REM compared to two other algorithms, namely, SSA and GA. This suggests that the LSC-SSA algorithm is well-suited for the specific challenges of sizing a microgrid incorporating various renewable energy sources.

The suggested REM configuration results in a total Annualized System Cost (ASC) of 1685672 million dollars (M$) and a Levelized Cost of Electricity (LCOE) of 0.927 dollars per kilowatt-hour ($/kWh). These economic indicators highlight the cost-effectiveness of the proposed hybrid REM design.

The overall finding from the conclusion underscores that the hybrid approach, integrating the LSC-SSA algorithm with rule-based supervisory EMS and sizing, leads to improved reliability and cost-effectiveness. This integration positions the proposed REM design as a promising alternative, offering enhanced performance and economic viability in comparison to traditional approaches.

Please note that emission analysis has not been incorporated into the study. This decision stems from the classification of biomass gasification, a key component of our proposed Hybrid Renewable Energy System (HRES), as a widely recognized renewable energy source. This classification is justified by the reliance of biomass gasification on organic materials and the carbon-neutral nature of the biomass carbon cycle.

Expanding the horizons of the study, the integration of electric vehicles (EVs) could also be a valuable addition. EVs could play a dual role in the system, acting as both a load and an additional storage unit. This dynamic inclusion adds complexity to the analysis, considering the interplay between the energy demand of the household, the energy storage capacity of EVs, and the potential benefits of bidirectional energy flow.

AKNOWLEGMENT

The authors express their sincere gratitude to Universiti Teknologi Malaysia (UTM) for granting access to their library facilities. Furthermore, they extend their heartfelt thanks to all those who have made contributions, either directly or indirectly, to the creation of this article.

REFERENCES

[1] A. K. Aliyu, B. Modu, and C. W. Tan, "A review of renewable energy development in Africa: A focus in South Africa, Egypt and Nigeria," *Renew. Sustain. Energy Rev.*, vol. 81, pp. 2502–2518, Jan. 2018.

[2] N. Bashir, B. Modu, and P. Harcourt, "Techo-economic analysis of off-grid renewable energy systems for rural electrification in North–Eastern Nigeria," *Int. J. Renew. Energy Res.*, vol. 8, no. 3, pp. 1217–1228, 1228.

[3] B. Modu, A. K. Aliyu, A. L. Bukar, M. Abdulkadir, Z. M. Gwoma, and M. Mustapha, "Techno-economic analysis of off-grid hybrid PV-diesel-battery system in Katsina State, Nigeria," *Arid Zone J. Eng., Technol. Environ.*, vol. 14, no. 2, pp. 317–324, 2018.

[4] A. Z. Arsad, M. A. Hannan, A. Q. Al-Shetwi, M. Mansur, K. M. Muttaqi, Z. Y. Dong, and F. Blaabjerg, "Hydrogen energy storage integrated hybrid renewable energy systems: A review analysis for future research directions," *Int. J. Hydrogen Energy*, vol. 47, no. 39, pp. 17285–17312, May 2022.

[5] A. L. Bukar, C. W. Tan, and K. Y. Lau, "Optimal sizing of an autonomous photovoltaic/wind/battery/diesel generator microgrid using grasshopper optimization algorithm," *Sol. Energy*, vol. 188, pp. 685–696, Aug. 2019.

[6] A. Kaabeche, S. Diaf, and R. Ibtiouen, "Firefly-inspired algorithm for optimal sizing of renewable hybrid system considering reliability criteria," *Sol. Energy*, vol. 155, pp. 727–738, Oct. 2017.

[7] O. Nadjemi, T. Nacer, A. Hamidat, and H. Salhi, "Optimal hybrid PV/wind energy system sizing: Application of cuckoo search algorithm for Algerian dairy farms," *Renew. Sustain. Energy Rev.*, vol. 70, pp. 1352–1365, Apr. 2017.

[8] A. Kaabeche, M. Belhamel, and R. Ibtiouen, "Techno-economic valuation and optimization of integrated photovoltaic/wind energy conversion system," *Sol. Energy*, vol. 85, no. 10, pp. 2407–2420, Oct. 2011.

[9] B. Modu, M. P. Abdullah, A. L. Bukar, M. F. Hamza, and M. S. Adewolu, "Operational strategy and capacity optimization of standalone solar-wind-biomass-fuel cell energy system using hybrid LF-SSA algorithms," *Int. J. Hydrogen Energy*, vol. 50, pp. 92–106, Jan. 2024.

[10] B. Modu, M. P. Abdullah, A. L. Bukar, and M. F. Hamza, "A systematic review of hybrid renewable energy systems with hydrogen storage: Sizing, optimization, and energy management strategy," *Int. J. Hydrogen Energy*, vol. 48, no. 97, pp. 38354–38373, Dec. 2023.

[11] M. M. Samy, M. I. Mosaad, and S. Barakat, "Optimal economic study of hybrid PV-wind-fuel cell system integrated to unreliable electric utility using hybrid search optimization technique," *Int. J. Hydrogen Energy*, vol. 46, no. 20, pp. 11217–11231, Mar. 2021.

[12] B. A. Bhayo, H. H. Al-Kayiem, S. I. U. Gilani, N. Khan, and D. Kumar, "Energy management strategy of hybrid solar-hydro system with various probabilities of power supply loss," *Sol. Energy*, vol. 233, pp. 230–245, Feb. 2022.

[13] A. E. Badoud, F. Merahi, B. Ould Bouamama, and S. Mekhilef, "Bond graph modeling, design and experimental validation of a photovoltaic/fuelcell/electrolyzer/battery hybrid power system," *Int. J. Hydrogen Energy*, vol. 46, no. 47, pp. 24011–24027, Jul. 2021.

[14] M. Jahannoosh, S. A. Nowdeh, A. Naderipour, H. Kamyab, I. F. Davoudkhani, and J. J. Klemeš, "New hybrid meta-heuristic algorithm for reliable and cost-effective designing of photovoltaic/wind/fuel cell energy system considering load interruption probability," *J. Cleaner Prod.*, vol. 278, Jan. 2021, Art. no. 123406.

[15] C. Zhang, J. Xia, X. Guo, C. Huang, P. Lin, and X. Zhang, "Multi-optimal design and dispatch for a grid-connected solar photovoltaic-based multigeneration energy system through economic, energy and environmental assessment," *Sol. Energy*, vol. 243, pp. 393–409, Sep. 2022.

[16] S. Ferahtia, H. Rezk, A. Djerioui, A. Houari, A. Fathy, M. A. Abdelkareem, and A. G. Olabi, "Optimal heuristic economic management strategy for microgrids based PEM fuel cells," *Int. J. Hydrogen Energy*, vol. 52, pp. 775–784, Jan. 2024.

[17] Y. Khawaja, I. Qiqieh, J. Alzubi, O. Alzubi, A. Allahham, and D. Giaouris, "Design of cost-based sizing and energy management framework for standalone microgrid using reinforcement learning," *Sol. Energy*, vol. 251, pp. 249–260, Feb. 2023.

[18] Y. Zhang, P. E. Campana, A. Lundblad, and J. Yan, "Comparative study of hydrogen storage and battery storage in grid connected photovoltaic system: Storage sizing and rule-based operation," *Appl. Energy*, vol. 201, pp. 397–411, Sep. 2017.
[19] G. Correa, F. Volpe, P. Marocco, P. Muñoz, T. Falagüerra, and M. Santarelli, "Evaluation of levelized cost of hydrogen produced by wind electrolysis: Argentine and Italian production scenarios," *J. Energy Storage*, vol. 52, Aug. 2022, Art. no. 105014.
[20] R. Hemmati, H. Mehrjerdi, and M. Bornapour, "Hybrid hydrogen-battery storage to smooth solar energy volatility and energy arbitrage considering uncertain electrical-thermal loads," *Renew. Energy*, vol. 154, pp. 1180–1187, Jul. 2020.
[21] M. S. Behzadi and M. Niasati, "Comparative performance analysis of a hybrid PV/FC/battery stand-alone system using different power management strategies and sizing approaches," *Int. J. Hydrogen Energy*, vol. 40, no. 1, pp. 538–548, Jan. 2015.
[22] J. L. Cox, W. T. Hamilton, and A. M. Newman, "Parametric analysis on optimized design of hybrid solar power plants," *Sol. Energy*, vol. 252, pp. 195–217, Mar. 2023.
[23] M. M. Kamal, I. Ashraf, and E. Fernandez, "Optimal sizing of standalone rural microgrid for sustainable electrification with renewable energy resources," *Sustain. Cities Soc.*, vol. 88, Jan. 2023, Art. no. 104298.
[24] J. Zhou and Z. Xu, "Optimal sizing design and integrated cost-benefit assessment of stand-alone microgrid system with different energy storage employing chameleon swarm algorithm: A rural case in Northeast China," *Renew. Energy*, vol. 202, pp. 1110–1137, Jan. 2023.
[25] D. Fares, M. Fathi, and S. Mekhilef, "Performance evaluation of metaheuristic techniques for optimal sizing of a stand-alone hybrid PV/wind/battery system," *Appl. Energy*, vol. 305, Jan. 2022, Art. no. 117823.
[26] M. M. Kamal, I. Ashraf, and E. Fernandez, "Planning and optimization of microgrid for rural electrification with integration of renewable energy resources," *J. Energy Storage*, vol. 52, Aug. 2022, Art. no. 104782.
[27] J. Jiang, R. Zhou, H. Xu, H. Wang, P. Wu, Z. Wang, and J. Li, "Optimal sizing, operation strategy and case study of a grid-connected solid oxide fuel cell microgrid," *Appl. Energy*, vol. 307, Feb. 2022, Art. no. 118214.
[28] H. M. Sultan, A. S. Menesy, S. Kamel, A. Korashy, S. A. Almohaimeed, and M. Abdel-Akher, "An improved artificial ecosystem optimization algorithm for optimal configuration of a hybrid PV/WT/FC energy system," *Alexandria Eng. J.*, vol. 60, no. 1, pp. 1001–1025, Feb. 2021.
[29] H. A. El-Sattar, H. M. Sultan, S. Kamel, T. Khurshaid, and C. Rahmann, "Optimal design of stand-alone hybrid PV/wind/biomass/battery energy storage system in Abu-Monqar, Egypt," *J. Energy Storage*, vol. 44, Dec. 2021, Art. no. 103336.
[30] M. Kharrich, S. Kamel, M. Abdeen, O. H. Mohammed, M. Akherraz, T. Khurshaid, and S. Rhee, "Developed approach based on equilibrium optimizer for optimal design of hybrid PV/wind/diesel/battery microgrid in Dakhla, Morocco," *IEEE Access*, vol. 9, pp. 13655–13670, 2021.
[31] J. Li, J. Zhao, Y. Chen, L. Mao, K. Qu, and F. Li, "Optimal sizing for a wind-photovoltaic-hydrogen hybrid system considering levelized cost of storage and source-load interaction," *Int. J. Hydrogen Energy*, vol. 48, no. 11, pp. 4129–4142, Feb. 2023.
[32] Z. Li, Y. Liu, M. Du, Y. Cheng, and L. Shi, "Modeling and multi-objective optimization of a stand-alone photovoltaic-wind turbine-hydrogen-battery hybrid energy system based on hysteresis band," *Int. J. Hydrogen Energy*, vol. 48, no. 22, pp. 7959–7974, Mar. 2023.
[33] M. M. Kamal and I. Ashraf, "Planning and optimization of hybrid microgrid for reliable electrification of rural region," *J. Inst. Eng. B*, vol. 103, no. 1, pp. 173–188, Feb. 2022.
[34] Y. Song, H. Mu, N. Li, and H. Wang, "Multi-objective optimization of large-scale grid-connected photovoltaic-hydrogen-natural gas integrated energy power station based on carbon emission priority," *Int. J. Hydrogen Energy*, vol. 48, no. 10, pp. 4087–4103, Feb. 2023.
[35] Z. Ma, T. Tian, Q. Cui, J. Shu, J. Zhao, and H. Wang, "Rapid sizing of a hydrogen-battery storage for an offshore wind farm using convex programming," *Int. J. Hydrogen Energy*, vol. 48, no. 58, pp. 21946–21958, Jul. 2023.
[36] H. Moradi, M. Esfahanian, A. Abtahi, and A. Zilouchian, "Optimization and energy management of a standalone hybrid microgrid in the presence of battery storage system," *Energy*, vol. 147, pp. 226–238, Mar. 2018.
[37] A. Arasteh, P. Alemi, and M. Beiraghi, "Optimal allocation of photovoltaic/wind energy system in distribution network using meta-heuristic algorithm," *Appl. Soft Comput.*, vol. 109, Sep. 2021, Art. no. 107594.
[38] S. Singh, P. Chauhan, and N. Singh, "Capacity optimization of grid connected solar/fuel cell energy system using hybrid ABC-PSO algorithm," *Int. J. Hydrogen Energy*, vol. 45, no. 16, pp. 10070–10088, Mar. 2020.
[39] B. Modu, M. P. Abdullah, A. L. Bukar, M. F. Hamza, and M. S. Adewolu, "Energy management and capacity planning of photovoltaic-wind-biomass energy system considering hydrogen-battery storage," *J. Energy Storage*, vol. 73, Dec. 2023, Art. no. 109294.
[40] S. Singh, M. Singh, and S. C. Kaushik, "Feasibility study of an islanded microgrid in rural area consisting of PV, wind, biomass and battery energy storage system," *Energy Convers. Manage.*, vol. 128, pp. 178–190, Nov. 2016.
[41] W. Zhang, A. Maleki, M. A. Rosen, and J. Liu, "Sizing a stand-alone solar-wind-hydrogen energy system using weather forecasting and a hybrid search optimization algorithm," *Energy Convers. Manag.*, vol. 180, pp. 609–621, Jan. 2019.
[42] M. Castañeda, A. Cano, F. Jurado, H. Sánchez, and L. M. Fernández, "Sizing optimization, dynamic modeling and energy management strategies of a stand-alone PV/hydrogen/battery-based hybrid system," *Int. J. Hydrogen Energy*, vol. 38, no. 10, pp. 3830–3845, Apr. 2013.
[43] T. Ma, M. Cintuglu, and O. Mohammed, "Control of hybrid AC/DC microgrid involving storage renewable energy and pulsed loads," *IEEE Trans. Ind. Appl.*, vol. 53, no. 1, pp. 567–575, 2016.
[44] S. Ayub, S. M. Ayob, C. W. Tan, M. Taimoor, L. Ayub, A. L. Bukar, and M. Z. Daud, "Analysis of energy management schemes for renewable-energy-based smart homes against the backdrop of COVID-19," *Sustain. Energy Technol. Assessments*, vol. 52, Aug. 2022, Art. no. 102136.
[45] A. S. O. Ogunjuyigbe, T. R. Ayodele, and O. A. Akinola, "Optimal allocation and sizing of PV/wind/split-diesel/battery hybrid energy system for minimizing life cycle cost, carbon emission and dump energy of remote residential building," *Appl. Energy*, vol. 171, pp. 153–171, Jun. 2016.
[46] T. R. Ayodele and A. S. O. Ogunjuyigbe, "Increasing household solar energy penetration through load partitioning based on quality of life: The case study of Nigeria," *Sustain. Cities Soc.*, vol. 18, pp. 21–31, Nov. 2015.

BABANGIDA MODU received the B.Eng. degree in electrical and electronic engineering from the University of Maiduguri, Maiduguri, Nigeria, in 2008, and the M.Eng. degree in electrical engineering (power) from Universiti Teknologi Malaysia, Johor Bahru, Malaysia, in 2016, where he is currently pursuing the Ph.D. degree in electrical engineering. He is involved in research work on energy management systems. His research interests include energy management and renewable energy optimization.

MD. PAUZI BIN ABDULLAH (Senior Member, IEEE) received the B.Eng. degree in electrical and electronic engineering from Universiti Tenaga Nasional (UNITEN), Malaysia, in 2002, and the M.Sc. degree in electrical power engineering and the Ph.D. degree from the University of Strathclyde, Glasgow, U.K., in 2003 and 2008, respectively. He is currently an Associate Professor with the Faculty of Engineering, Universiti Teknologi Malaysia (UTM). He is also the Director with the Institute of Future Energy (IFE), UTM. His research interests include power systems analysis, systems security, deregulated electricity market, and demand-side management.

ABDULRAHMAN ALKASSEM (Member, IEEE) received the bachelor's degree in electrical engineering from Umm Al-Qura University, Saudi Arabia, in 2008, and the master's degree in electrical engineering and the Ph.D. degree in systems engineering from Concordia University, Canada, in 2012 and 2018, respectively. He is currently the Dean of the Faculty of Engineering and an Associate Professor with the Department of Electrical Engineering, Islamic University of Madinah. He has published several research articles and conferences in renewable energy sources planning, techno-economic analysis, and optimization. His research interests include renewable energy strategic planning, multi-criteria decision-making, energy efficiency, and sustainable development.

HASSAN Z. AL GARNI (Member, IEEE) received the M.E. degree in electrical and computer engineering and the Ph.D. degree in systems engineering from Concordia University, Canada, in 2013 and 2018, respectively. He is currently an Assistant Professor with the Department of Electrical Engineering, Jubail Industrial College-Royal Commission for Jubail and Yanbu, Saudi Arabia. He served in many administrative positions at the Jubail Industrial College, including the Chairperson of the Department of Electrical Engineering and the Deputy for Planning and Development. He has published many research articles and conference proceedings in the area of renewable energy. His employment experience includes working in instrumentation and control at SABIC for five years and teaching at the Jubail Industrial College for 14 years. His research interests include renewable energy (including solar photovoltaic planning, design, and optimization), soiling impact, site selection, panel orientation, and tracking systems. He was awarded the Concordia Accelerator Award, in 2018, the Concordia University Conference and Exposition Award, from 2017 to 2018, and the IEEE-SMC Travel Grant Award, in 2017.

MISHAAL ALKABI (Member, IEEE) received the bachelor's degree in electrical engineering from Umm Al-Qura University, Saudi Arabia, in 2008, and the master's degree in electrical engineering from Concordia University, Canada, in 2015. He is currently a Lecturer with the Department of Electrical Engineering, Umm Al-Qura University. His research interests include modeling and control with applications to microgrids, power electronics, and machines.